Applied Microbiology and Biotechnology (2024) 108:448
https://doi.org/10.1007/s00253-024-13283-3

METHODS AND PROTOCOLS

Harnessing sulfur-binding domains to separate *Sp* and *Rp* isomers of phosphorothioate oligonucleotides

Fulin Ge[1] · Yuli Wang[1] · Jinling Liu[1] · Hao Yu[1] · Guang Liu[1] · Zixin Deng[1] · Xinyi He[1]

Received: 8 June 2024 / Revised: 9 August 2024 / Accepted: 14 August 2024 / Published online: 27 August 2024

Abstract

Chemical synthesis of phosphoromonothioate oligonucleotides (PS-ONs) is not stereo-specific and produces a mixture of *R*p and *S*p diastereomers, whose disparate reactivity can complicate applications. Although the current methods to separate these diastereomers which rely on chromatography are constantly improving, many *R*p and *S*p diastereomers are still co-eluted. Here, based on sulfur-binding domains that specifically recognize phosphorothioated DNA and RNA in *R*p configuration, we developed a universal *s*eparation system for *p*hosphorothioate *o*ligonucleotide *i*somers using immobilized *S*BD (SPOIS). With the scalable SPOIS, His-tagged SBD is immobilized onto Ni-nitrilotriacetic acid-coated magnetic beads to form a beads/SBD complex, *R*p isomers of the mixture can be completely bound by SBD and separated from *S*p isomers unbound in liquid phase, then recovered through suitable elution approach. Using the phosphoromonothioate single-stranded DNA as a model, SPOIS separated PS-ON diastereomers of 4 nt to 50 nt in length at yields of 60–90% of the starting *R*p isomers, with PS linkage not locating at 5' or 3' end. Within this length range, PS-ON diastereomers that co-eluted in HPLC could be separated by SPOIS at yields of 84% and 89% for *R*p and *S*p stereoisomers, respectively. Furthermore, as each *R*p phosphorothioate linkage can be bound by SBD, SPOIS allowed the separation of stereoisomers with multiple uniform *S*p configurations for multiple phosphorothioate modifications. A second generation of SPOIS was developed using the thermolabile and non-sequence-specific SBD_{Ped}, enabling fast and high-yield recovery of PS substrate stereoisomers for the DNAzyme Cd16 and further demonstrating the efficiency of this method.

Key points

- *SPOIS allows isomer separations of the Rp and Sp isomers co-eluted on HPLC.*
- *SPOIS can obtain Sp isomers with 5 min and Rp in 20 min from PS-ON diastereomers.*
- *SPOIS was successfully applied to separate isomers of PS substrates of DNAzyme.*

Keywords Protein-DNA interaction · Microbial DNA binding protein · Sulfur-binding domain · Phosphorothioate oligonucleotide · Affinity-based oligo purification · Thermolabile protein

Introduction

Phosphoromonothioate (PS) modification of oligo(deoxy) nucleotides (ONs) is the substitution of a non-bridging oxygen atom in the phosphate group with a sulfur atom (Eckstein 1985), and PS modification is naturally present in the genomes of some bacteria and archaea (Zhou et al. 2005). PS-linkages are stable against nucleases (Potter and Eckstein 1984) and confer PS-ONs with improved cell penetration properties (Eckstein 2014), benefiting antisense strategies in which an ON can be designed to induce ribonuclease H (RNase H)-mediated cleavage of a target RNA. Several therapeutic PS-ONs exhibit promising activity that their unmodified ON analogues cannot achieve (Eckstein 1985; Yu et al. 2000). To date, ten of the eighteen approved ON drugs have PS modification sites (Egli and Manoharan 2023).

PS modification generates a chiral center at the phosphorous atom, producing a mixture of *R*p and *S*p diastereomers

✉ Xinyi He
xyhe@sjtu.edu.cn

[1] State Key Laboratory of Microbial Metabolism, Joint International Research Laboratory of Metabolic & Developmental Sciences, School of Life Sciences & Biotechnology, Shanghai Jiao Tong University, 800 Dongchuan Road, Shanghai 200240, People's Republic of China

in non-stereo-controlled chemical synthesis. Single-stranded (ss) PS-ONs pair with the complementary strand to form double-stranded (ds) PS-ONs, where the sulfur substituent on the chiral phosphorus atom faces either the inside (*R*p) or outside (*S*p) of the duplex. The PS stereoisomers exhibit distinct physical and biochemical properties. Stereochemically pure PS-ONs show different reactivities with nucleases. For example, as a key nuclease in the RNA interference pathway, RNase H is recruited more efficiently by antisense PS-ONs in *R*p than in *S*p configuration, but shows lower endonuclease activity toward PS linkages in *S*p than in *R*p configuration (Koziolkiewicz et al. 1995). Additionally, DNA polymerase I (Brautigam and Steitz 1998) and snake venom phosphodiesterase (Yu et al. 2000) exhibited lower exonuclease activity when PS sites were in the *S*p configuration than *R*p configuration. By contrast, PS-DNA with the *R*p configuration had improved resistance to exonuclease III (Putney et al. 1981) and nuclease P1 (Potter et al. 1983) than *S*p configuration.

There is growing interest in the synthesis of enantiopure PS-ONs. To this end, "stereo-controlled liquid phase synthesis of phosphorothioate oligonucleotides on a soluble support" chemical synthesis methods were developed (Guo et al. 1998; Oka et al. 2008; Stec et al. 1998; Wilk et al. 2000). Subsequently, the stereo-specific PS synthesis of antisense oligonucleotide drug molecules via nucleoside 3′-oxazaphospholidine derivatives by stereocontrolled oligonucleotide synthesis with iterative capping and sulfurization (SOSICS) was accomplished (Iwamoto et al. 2017). However, these methods have problems with low efficiency, insufficient selectivity, and difficulty in removing chiral auxiliaries after synthesis. In an alternative approach, the separation of diastereomers has been employed to obtain enantiopure PS-ONs after chemical synthesis. Initially, *R*p-specific snake venom phosphodiesterase and *S*p-specific nuclease P1 were used to remove the unwanted stereoisomers (Bryant and Benkovic 1979). With the development of chromatography, ion-exchange or reversed-phase liquid chromatography was applied in separation of diastereomers with one or more PS sites (Frederiksen and Piccirilli 2009; Murakami et al. 1994). Currently, PS-ON diastereomers with more PS sites are mainly resolved and purified by ion-pair reversed-phase liquid chromatography (Enmark et al. 2020, 2021). HPLC systems can provide a visualization window to monitor the separation process in real time, as well as to calculate the yield of PS-ONs easily. However, HPLC separation of PS-ONs faces two practical challenges: the first one is that some diastereomers even with one PS site, co-elute or elute within a short time interval, leading to failure in separation or requirement for multiple runs of separation, respectively. Secondly, the development of an individually customized separation procedure for a given set of PS-ON diastereomers is required. These shortcomings in stereoisomer separation by HPLC can involve substantial costs in labor and time, and therefore, there is an increasing need to develop a universal technique for the rapid separation of PS-ON diastereomers.

We previously discovered a superfamily of sulfur-binding domains (SBDs) that specifically bind only PS-dsDNA in the *R*p configuration (Hu et al. 2023; Liu et al. 2018; Yu et al. 2020) with an equilibrium dissociation constant value (K_D) of 5.55 nM ~ 1 μM (Yu et al. 2020, 2018). Here, we report that SBD_{Ana}, the SBD region isolated from the PS-DNA-specific PD-(D/E) XK nuclease (WP_041454130.1) from *Anaeromyxobacter* sp. K, is able to bind versatile types of PS-ONs with an improved affinity toward ssDNA and single-stranded RNA (ssRNA) when compared with two other characterized SBDs. This feature of SBD_{Ana} was employed to develop a universal separation system for PS-ON diastereomers based on His-tagged SBD_{Ana} immobilized by Ni-nitrilotriacetic acid (NTA)–coated magnetic beads, and we have named this system "SPOIS" for *s*eparation system for *p*hosphorothioate *o*ligonucleotide *i*somers using immobilized *S*BD. Using phosphoromonothioate ssDNA as the model, SPOIS could separate (i) PS-ON diastereomers of 4–50 nt in length, with yields above 60%; (ii) co-eluting diastereomers, with an 84% yield of *R*p stereoisomers and 89% yield of *S*p stereoisomers; and (iii) diastereomers bearing two or three PS sites, with a 40–50% yield of uniform *S*ps. Based on SBD screening, SPOIS-II, the upgraded version of SPOIS, was developed to simplify the elution process using SBD_{Ped}, a truncated protein from the PS-DNA-specific HNH endonuclease (WP_088299980.1) from *Pedobacter* sp. AJM, with only 5 min required for separation of *S*p isomers and 20 min for *R*p isomers. We successfully applied SPOIS-II to the separation of diastereomers of PS substrates for DNAzymes. The establishment of SPOIS provides a universal and effective way to separate diastereomers for PS-ON with one PS site, also proposes the possibility of separating diastereomers for PS-ON with more PS sites by bioenzymatic approach.

Methods and materials

Reagents and materials

The ssDNA or ssRNA ONs (Table S1) and the gene fragments encoding the functional SBD_{Ana} and SBD_{Ped} were synthesized by GENEWIZ (Suzhou, China). dsDNA oligonucleotides were obtained by annealing two equimolar, complementary ssDNA strands. HisSep Ni–NTA MagBeads were purchased from Yeasen (Shanghai, China). Chemicals and reagents were analytical grade and dissolved in double-distilled water prepared by the Milli-Q Water Purification System (Millipore, USA).

Plasmid construction and protein purification

The primers and gene fragments used in this study are listed in Table S2. The DNA fragment encoding SBD_{Ana} or SBD_{Ped} was cloned into the *Nde*I and *Xho*I site of pET28a, and the recombinant plasmid was transformed into *Escherichia coli* BL21 (DE3). A 10 mL overnight culture of the recombinant strain BL21 /pET28a-SBD_{Ana} or BL21/pET28a-SBD_{Ped} was inoculated into 1 L liquid LB medium supplied with 50 μg/mL kanamycin, which was then cultured at 37 ℃ (220 rpm) to OD600 0.6, cooled to room temperature, and IPTG was added to a final concentration of 0.2 mM, followed by the sequential culture for 20 h (220 rpm) at 16 ℃. Cells were collected and resuspended in binding buffer (20 mM Tris–HCl, pH 8.0, 300 mM NaCl, 50 mM imidazole, 10% glycerol), and lysed by a high-pressure homogenizer (UH-06, Union-Biotech). After centrifugation at 15,000 rpm for 15 min, the supernatant was applied to a pre-equilibrated 2.5 mL Ni–NTA column (GE Healthcare) and washed with 50-column volume of the binding buffer prior to protein elution with elution buffer (20 mM Tris–HCl, pH 8.0, 300 mM NaCl, 500 mM imidazole, 10% glycerol). The eluted protein was further purified by removing genomic DNA fragments using HiTrap Q HP (GE Healthcare) and finally desalted by a PD-10 desalting column (GE Healthcare) and stored in desalting buffer (20 mM Tris–HCl, pH 8.0, 300 mM NaCl, 10% glycerol) at − 30℃. Protein concentration was determined using CBB Staining Solution (Tiangen).

Preparation of PS oligonucleotide isomers

The *R*p and *S*p stereoisomers of single-stranded PS-ONs were separated by anion exchange HPLC with a DNAPac PA-100 analytical column (Thermo, 4 mm I.D. × 250 mm, 13 μm) on an Agilent 1260 Infinity Series system at a flow rate of 0.8 mL/min with the following parameters: column at 55 ℃; solvent A, 10 mM Tris–HCl, pH 8.0; solvent B, 10 mM Tris–HCl, pH 8.0, 1 M NaCl; gradient, 0% B to 100% B over 40 min; detection by UV absorbance at 260 nm. The eluent was desalted with a Copure C18 column (Biocomma), lyophilized in 50% methanol in an Alpha 2–4 LSCbasic freeze-dryer (CHRIST), and dissolved in double-distilled water. The hemi-PS dsDNA was generated by annealing of an *R*p or *S*p stereoisomer with its complementary unmodified DNA strand in equimolar concentrations.

Electrophoretic mobility shift assays (EMSAs)

A 10 μL EMSA reaction mixture contained 10 pmol DNA or RNA and 40 pmol protein in binding buffer (20 mM Tris–HCl, pH 8.0, 100 mM NaCl, 5% glycerol); for RNA, 1 mM DTT and 1 μL RNase inhibitor (Takara Bio Inc) were extra added. After incubation on ice for 10 min, the mixtures were loaded onto 12% native polyacrylamide gels and electrophoresed for 30 min in an ice bath at 15 mA in 1 × TAE buffer. The gels were stained with 1 × SYBR Gold (S11494, Thermo-Fisher Scientific) for 5 min before being imaged on a Bio-Rad GelDoc XR + (Bio-Rad).

Separation process for SPOIS

Basically, a typical SPOIS procedure utilized magnetic beads (20561ES03, Yeasen) with Ni–NTA covalently modified surface. The ethanol solvent was removed from the magnetic bead suspension (20 μL) by magnetic adsorption, and the beads were transferred to the binding reaction system (40 nmol His-tagged SBD, 1 nmol synthetic PS-ONs consisting of both *R*p and *S*p stereoisomers, 10 mM Tris–HCl, pH 8.0, 100 mM NaCl) in a final volume of 200 μL. The binding reaction was performed on a multipurpose roto-shaker (20 circles per minute, QB-206, Kylin-Bell) at room temperature for 5 min, followed by separation of the magnetic beads from the solution by a magnetic rack. The solution containing *S*p PS-ONs (unbound) was transferred, and the beads were washed twice with washing buffer (10 mM Tris–HCl, pH 8.0, 100 mM NaCl). For SPOIS-I, to obtain the SBD_{Ana}/*R*p PS-ON complex, an imidazole solution (500 mM imidazole, 10 mM Tris–HCl, pH 8.0, 100 mM NaCl) was applied to the washed beads. Next, to obtain the *R*p PS-ONs, the sample was heated at 60 °C for 10 min followed by centrifugation at 12,000 g for 5 min; the supernatant was collected and then desalted by a Copure C18 column (Biocomma). For SPOIS-II, the *R*p PS-ONs were directly eluted from the magnetic bead/SBD_{Ped} complex by heating at 85 °C for 10 min.

Electrophoresis and HPLC analysis of oligonucleotide products by SPOIS

To monitor the purity and concentration of ONs in each separation step for SPOIS, 10 μL samples from the above steps (binding, removal of unbound material, elution by imidazole, elution by heating) were loaded onto 12% native polyacrylamide gels and electrophoresed for 30 min in an ice bath at 15 mA in 1 × TAE buffer. The gel was stained with 1 × SYBR Gold (S11494, Thermo-Fisher Scientific) for 5 min for imaging. At the same time, 100 μL (< 100 pmol) of each sample was injected into an HPLC system with the same methods used as in preparation of the PS-ON isomers. The quantification of the samples was based on the peak area obtained by HPLC analysis, and the specific calculations were as follows:

Actual yield (*R*p) peak area of *R*p isomer in eluate/ peak area of *R*p isomer in PS-ON;

Actual yield (*S*p) peak area of *S*p isomer in unbound/ peak area of *S*p isomer in PS-ON

Specifically, for the analysis of PS-4 nt-2(AG*GC) (Fig. 3A, Figure S7) whose *R*p and *S*p diastereomers cannot be distinguished by HPLC, the *S*p isomer yields in the unbound portion were set at 100% to calculate the yield of *R*p isomers in the eluate. The same calculation was also applied in Fig. 3B and Figure S9 except that the *S*p isomer yield in the unbound portion was calibrated by systematic yield based on non-PS-ONs.

DNAzyme cleavage assays

Gel-based DNAzyme cleavage assays were performed according to the method of Huang and Liu (2015). Essentially, 0.7 μM fluorescein-labeled PS substrate was annealed with 1.1 μM Cd16 DNAzyme in buffer B (50 mM MES, pH 6.0, 25 mM NaCl). Cd^{2+} measuring 10 μM was added to initiate the cleavage, and after a 60 min reaction time, the cleavage products were loaded onto a 12% native polyacrylamide gel with 1 × DNA Loading Buffer (P0220, Vazyme) and electrophoresed for 30 min at 10 mA in 1 × TAE buffer. The analysis was based on the gel imaging on a Bio-Rad GelDoc XR + (Bio-Rad) and Image Lab Software (Bio-Rad).

Results

SBD_{Ana} has high binding affinity for single-stranded *R*p PS-ONs

We previously reported the crystal structures of SBDs complexed with *R*p DNA duplexes with PS linkages at various positions in the sequences (Hu et al. 2023; Liu et al. 2018; Yu et al. 2020). However, ssPS-ONs are used more frequently in various applications. Through preliminary screening by EMSA, an SBD named SBD_{Ana} from *Anaeromyxobacter* sp. K (SBD#9 in Table S3) showed an obviously higher binding affinity for ssPS-ONs when compared to SBD_{Hga} and SBD_{Spr} (Fig. 1, Figure S1B), both of which firmly bind to dsPS-ONs with an equilibrium dissociation constant of ~ 5 nM (Hu et al. 2023; Yu et al. 2020). Notably, SBD_{Ana} could effectively discern the *R*p PS-ONs from the *S*p PS-ONs and non-PS-ONs, either as DNA or RNA, as evidenced by the absence of shifted bands for the *S*p and non-PS forms of ONs (Fig. 1). Structural prediction and interaction analyses revealed that, consistent with the published binding models of SBDs and PS dsDNA, the binding of SBD_{Ana} and PS ssDNA relied primarily on a sulfur-binding cavity consisting of Y27, K28, Y78, P79, and H82, supplemented by hydrogen bonds, electrostatic interactions, and hydrophobic interactions with the phosphate backbone and bases of the PS ssDNA to form a stable complex (Figure S1C). Given its stereo- and PS-specific activity, SBD_{Ana} is a promising protein tool for separation of PS-ON diastereomers, although the applications may be broader with DNA as our data suggest that SBD_{Ana} has a greater affinity for DNA PS-ONs than for RNA PS-ONs.

An SBD_{Ana}-based SPOIS system for separation of PS-ON diastereomers

Magnetic beads are typically used for rapid separation of solid and liquid phases. The magnetic beads used here, with a medium particle diameter of 30 μm, are based on 4% cross-linked agarose coupled with tetra-coordinated NTA and form a stable octahedral structure after chelating Ni^{2+}. SBDs carrying a poly-histidine tag at the N-terminal will be anchored by coordination bonds between histidine residues and Ni^{2+}. Also, the attachment can be abolished by competition with imidazole (Figure S2). In order to establish our *s*eparation system for *p*hosphorothioate *o*ligonucleotide *i*somers based on immobilized *S*BD_{Ana} (SPOIS), the saturation dosage of magnetic beads, SBD_{Ana}, and PS-ONs needed to be defined. Based on the instruction manual for the magnetic beads, the minimal His-tagged SBD_{Ana} loading capacity for 1 μL Ni–NTA-coated magnetic beads would be 2.11 nmol. Therefore, for each 1 nmol SBD_{Ana}, 0.5 μL magnetic beads were added to allow for complete binding (Figure S3). To evaluate the capture rate of SBD_{Ana} for *R*p PS-ONs with this parameter, 1 nmol *R*p PS-ON was added to different amounts of the bead-bound SBD_{Ana}. We determined that, for each 1 nmol *R*p PS-ON to be completely captured, more than 40 nmol SBD_{Ana} was needed (Figure S3).

The whole process for the SPOIS system is depicted in Fig. 2A. Briefly, His-tagged SBD is immobilized onto the Ni–NTA-coated magnetic beads to form a magnetic beads/SBD complex, and then an appropriate molar amount of PS-ON stereoisomers is mixed with the magnetic beads/SBD. The *R*p stereoisomers will be specifically bound and tethered by the immobilized SBD (step 1, Fig. 2A), whereas the unbound *S*p isomers are directly recovered from the liquid phase (step 2a, Fig. 2A). To elute the SBD-bound *R*p PS-ONs, we firstly heat-treated the washed complex of the magnetic beads/SBD/*R*p PS-ONs (step 2b, Fig. 2A) in washing buffer at 95 °C for 30 min. However, less than 10% of the starting *R*p PS-ONs was recovered (Figure S4). Alkali treatment also failed to improve recovery. Although *R*p-ONs achieved a *ca.* 85% yield after chloroform extraction of SBD_{Ana}, chloroform can be harmful to the user and is environmentally unfriendly. As an alternative, we attempted to elute the SBD/*R*p PS-ON complex from the magnetic beads with an imidazole solution (step 3, Fig. 2A, Figure S4), followed by heat treatment optimized at 60 °C for 10 min

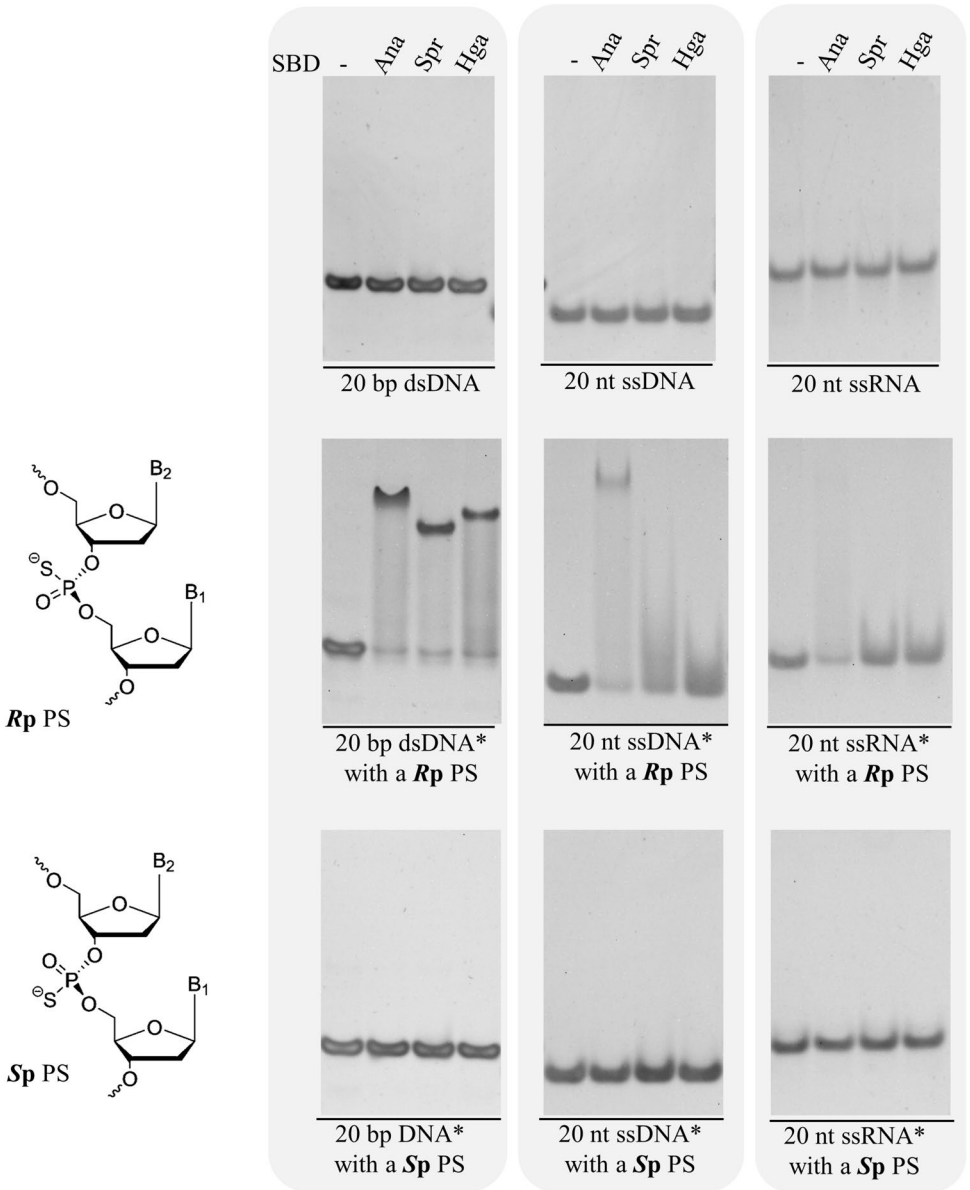

Fig. 1 The stereo-specific SBD_{Ana} has high binding affinity for PS-ONs. SBDs Ana, Spr, and Hga constitute the first 165, 165, and 160 aa residues, respectively, of phosphorothioate-dependent restriction enzymes from the respective bacteria *Anaeromyxobacter* sp. K (WP_041454130.1), *Streptomyces pristinaespiralis* (WP_005318208.1), and *Hahella ganghwensis* (WP_020410240.1), where the accession numbers refer to the associated enzyme. Each EMSA was performed with an SBD to DNA or RNA molar ratio of 4:1. PS denotes the phosphoromonothioate group. *R*p and *S*p stereoisomers were resolved by HPLC with reference to Figure S1A. "-" represents controls without SBD added

(Figure S5) to release the *R*p PS-ONs from the SBD (step 4, Fig. 2A), achieving a yield of more than 80%. The *R*p PS-ONs were then purified by centrifugation and desalting to remove denatured SBD and imidazole (step 5, Fig. 2A).

SPOIS separation of stereochemically pure PS-ONs is performed in a liquid phase. Since the conditions for SBD binding of PS-ONs in EMSAs and liquid are different, the binding affinity of SBD_{Ana} for different types of PS-ONs may also differ between EMSAs and liquid phase analysis. We therefore examined the binding stereospecificity and capacity of SBD_{Ana} for *R*p and *S*p stereoisomers of PS-ONs in ssDNA, dsDNA, and RNA forms, with separation of the chemically synthesized PS-ONs conducted by HPLC. Equimolar amounts of *R*p and *S*p stereoisomers and corresponding non-PS controls were mixed and separated by SPOIS with or without SBD_{Ana} loaded, and then the purity and yield of the purified *R*p and *S*p stereoisomers were analyzed. It is worth noting that as the control SPOIS without SBD_{Ana} loaded, the results indicated that all ONs appeared in Unbound rather than Eluate, with no significant decrease compared to starting ONs (Figure S6A), which excluded the possibility that the binding of magnetic beads coated with Ni–NTA for ONs led to a decrease in the yield. When SBD_{Ana} was loading on SPOIS, our results indicated that only *R*p isomers could be bound by SBD, with no binding of *S*p isomers or non-PS controls regardless of the nucleic acid form of the ONs (Fig. 2B, Figure S6B), demonstrating that SPOIS is *R*p stereo-specific. For 20 bp PS-dsDNA, the yield of *R*p isomers separated by SPOIS was about 77%, and that of *S*p isomers was up to 82%. For 20 nt PS-ssDNA, the

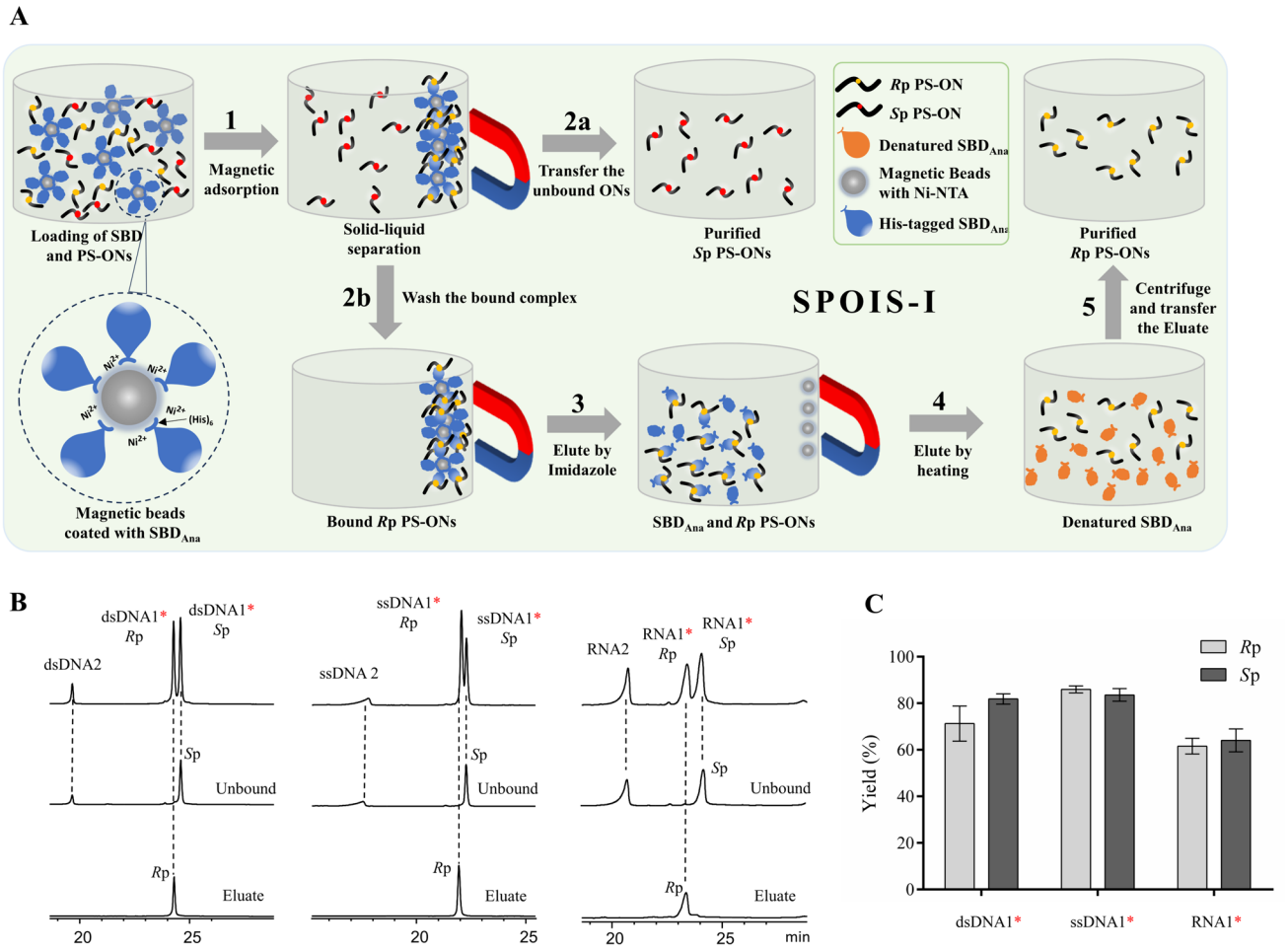

Fig. 2 Development of the PS- and stereo-specific SPOIS-I process for separation of PS-ON diastereomers. **A** Flowchart of the SBD_{Ana}-based SPOIS-I separation process. **B** HPLC analysis of the separation products from SPOIS. The top of each graph is the mixture with oligonucleotide plus its synthetic PS-ON diastereomers. The empirical rule suggests that the first and second peaks correspond to *R*p and *S*p diastereomers, respectively (Frederiksen and Piccirilli 2009). "Unbound" in the middle of each graph corresponds to *S*p PS-ONs that were not bound by SBDs after step 2a in panel A, and "Eluate" denotes the purified *R*p PS-ONs after step 5. "*" represents the PS linkage; sequences for these PS-ONs are listed in Table S1. **C** Quantitative analysis of the *R*p and *S*p diastereomer yields for different types of substrates. Calculations were performed using the data shown in panel **B**. Error bars represent the standard deviations of yields performed in triplicate

yields of *R*p and *S*p isomers were both around 85%, and for 20 nt PS-RNA, the yields of *R*p and *S*p isomers decreased slightly to 61% and 64%, respectively (Fig. 2C). These data demonstrated that SPOIS-I is a promising, device-free system for PS-ON stereoisomer separation with binding stereospecificity for *R*p configuration.

PS-ON substrate length for efficient separation of diastereomers by SPOIS

To determine the application range for SPOIS-I in terms of substrate length, chemically synthesized ssPS-ONs of varied lengths were used as SPOIS substrates, and the yield of each *R*p PS-ON was measured. We started with an 8 nt PS-ON (CGAG*GCCG, "*" denoting PS linkage), the shortest length that we had tested for binding by SBDs in previous work (Yu et al. 2020). The following PS-ONs were also synthesized and applied to the SPOIS-I: 2 nt (G*G), 3 nt-1(G*GC), 3 nt-2 (AG*G), 4 nt-1(G*GCC), 4 nt-2 (AG*CC), and 6 nt (GAG*GCC). For each PS-ON, the bound fraction was eluted and analyzed by HPLC along with the starting PS-ON diastereomers (Figure S7). Results indicated that the PS-ONs G*G, G*GC, AG*G, and G*GCC could not be bound by the SBD as the elution fraction gave no peak in the HPLC profile. For AG*GC (4 nt-2), a peak corresponding to the *R*p stereoisomer in the starting PS-ON diastereomers appeared with a yield of *ca.* 60% after separation. By comparison, the yield of *R*p isomer increased notably to 85% and 88% for 6 nt and 8 nt PS-ONs, respectively (Fig. 3A).

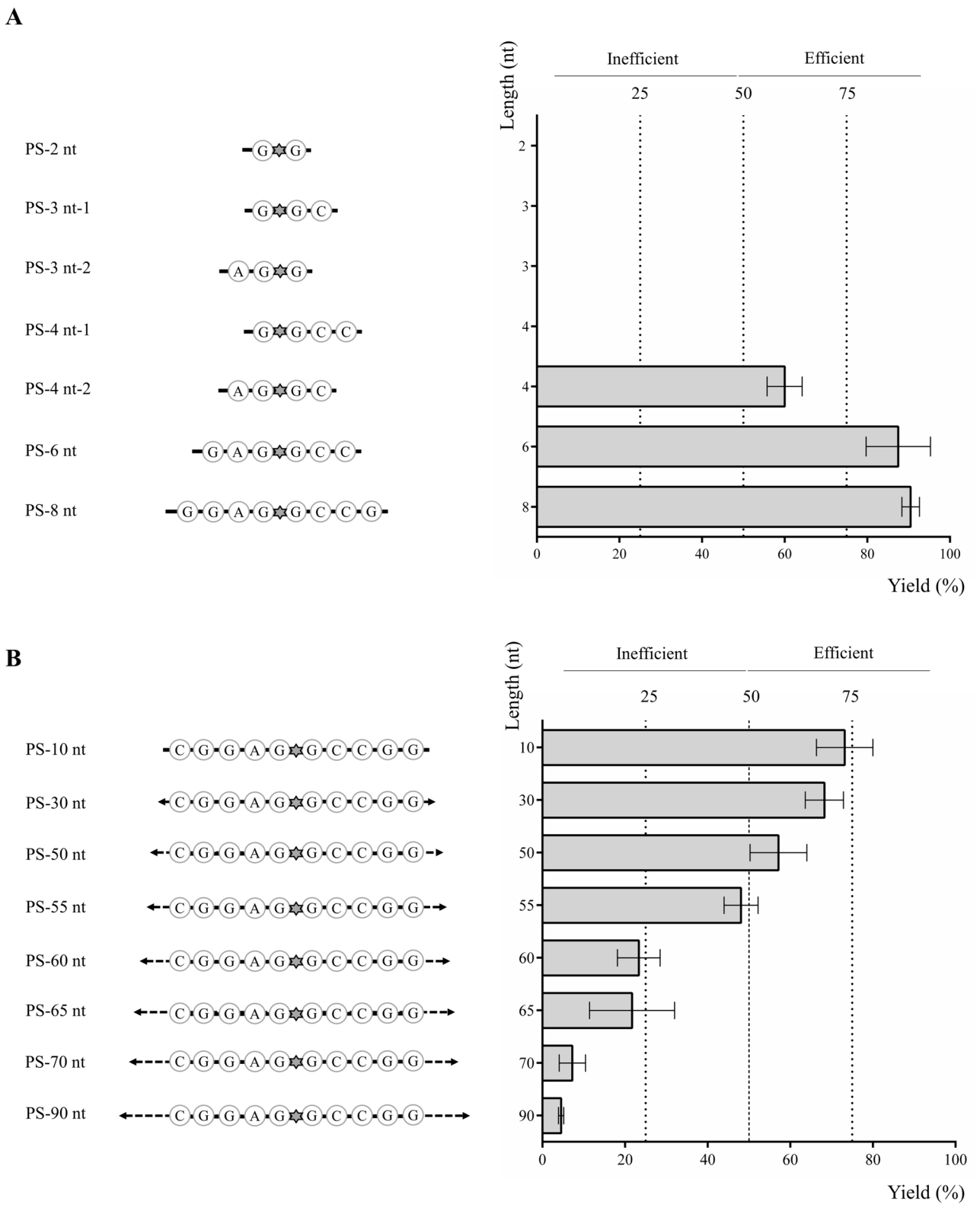

Fig. 3 Impact of ssPS-ON length on separation efficiency of SPOIS. **A** Analysis with short PS-ONs of 2–8 nt in length. The central sequences bearing the PS linkage in the PS-ONs are indicated. **B** Analysis with PS-ONs of 10–90 nt. The sequences and position of PS linkages for all PS-ONs are listed in Table S1. Calculations of separation efficiency were performed using the data shown in Figures S7 and S9. Error bars represent the standard deviations of yields performed in triplicate

Based on the complex structure of SBDs with their respective PS-ONs, in addition to interactions with the sulfur atom in PS-ONs, SBDs bond with the phosphodiester backbone and bases adjacent to the PS linkage (Figure S8). These interactions may also be necessary for firm binding of PS-ONs by SBD_{Ana}. These observations demonstrated that the minimum length for efficient isolation of PS-ON isomers by SPOIS is 4 nt, which should include a phosphodiester bond linkage flanking each side of the central PS linkage.

Additionally, six PS-ONs with lengths spanning from 10 to 90 nt centered around a G*GCC sequence were individually examined for *R*p isomer yield. Unexpectedly, the *R*p and *S*p isomers of each synthetic PS-ON co-eluted in one peak in HPLC chromatography (Figure S9). Therefore, we included the corresponding non-PS-ONs, which eluted as a distinct peak at an earlier time than the PS-ONs (Figure S9), accompanied by a later peak that should correspond to *S*p PS-ONs in the unbound fraction. Accordingly, the PS-ONs in the peak eluted from the bound fraction should correspond to *R*p PS-ONs. The yield of the *R*p isomers remained at 57 ~ 73% when PS-ONs were 10 to 50 nt in length, but sharply decreased from 48 to 23% when the length increased from 55 to 60 nt, and PS-ONs with a length longer than 70 nt gave a yield of below 10% (Fig. 3B). Taken together, these results indicated that the optimal length for efficient separation of PS-ON *R*p isomers ranges from 4 to 55 nt.

Application of SPOIS for separation of chemically synthesized PS-ON stereoisomers

The diastereomer separation of PS-ONs with one PS site has become easier with advances in chromatographic techniques, but it should not be neglected that there are still a large number of PS-ONs that co-elute or elute within a short time interval, making them difficult to be completely separated on chromatogram, which requires more optimizations of HPLC conditions. By contrast, one of the advantages of universal SPOIS is to address this issue. To demonstrate this capacity, a PS-ON ssDNA4* with two diastereomers that co-elute in HPLC was applied to SPOIS-I (Table 1). The first, second, and fourth fractions gave bands of the same size on the gel whereas the third fraction, corresponding to the SBD_{Ana}/*R*p PS-ON complex eluted by imidazole, resolved as a different, shifted band (Fig. 4A). In contrast, the HPLC profile showed that separation of the ssDNA4* diastereomers by HPLC was not feasible. With SPOIS, the unbound fraction produced a peak corresponding to its *S*p isomers, and the eluate fraction produced the peak for the *R*p isomers. Mixing the unbound and eluate fractions reproduced the peak pattern consistent with the starting PS-ON (Fig. 4A), validating the feasibility of SPOIS for the separation of diastereomers that co-elute by HPLC.

Most of the approved antisense PS-ON drugs, such as mipomersen (Roberts et al. 2020), feature multiple chiral PS linkages. However, it is currently not possible to resolve all diastereoisomers of ONs with more than four or five PS sites (Enmark et al. 2020). As a preliminary exploration, the effectiveness of SPOIS in the purification of PS-ONs bearing two or three tandem PS sites was examined (Fig. 4B, Table 1). As the binding mode of the SBD to both starting substrates is similar, for simplicity we only describe the results here based on substrates with two tandem PS linkages. Upon separation by SPOIS-I, the unbound fraction produced a band with relatively low intensity on the gel, and by comparison, the eluate fraction generated a band with much higher intensity. HPLC analysis revealed that the peak with the latest retention time of the starting PS-ONs disappeared in the profile for the eluate and was present in the unbound fraction. Based on the empirical rule, the PS-ONs in this peak are *S*p*S*p isomers. By comparison, PS-ONs in the peaks for the eluate fraction contain at least one *R*p linkage. These findings indicate that the SPOIS system can effectively separate stereo-pure PS-ONs with uniform *S*ps.

Identification of a thermolabile and *R*p-specific SBD_{Ped} to establish SPOIS-II

The elution method adopted in SPOIS-I was laborious and uneconomical. To shorten the elution process after step 2b in SPOIS-I, we wanted to screen for an SBD homolog that would have PS-ON binding features similar to SBD_{Ana} at room temperature but that would also be easily denatured by heat treatment to release *R*p isomers when bound to magnetic beads via His-Ni–NTA pairing. In a screen of SBD_{Ana} homologs with similar affinity, sequence specificity, and type of PS-ON binding substrate, but with a different thermostability, 29 soluble SBDs were obtained out of 77 putative SBDs (Table S3, Table S4). For further screening of the thermolabile homologs, the SBDs were incubated at 56 °C for 1 h, conditions that were slightly modified from a general routine lab procedure in which heat inactivation of target protein was performed at 55 °C for 30 min (Cancado et al.

Table 1 Yield of *R*p and *S*p (*S*p*S*p/*S*p*S*p*S*p) after SPOIS[#]

PS-ON	*R*p yield (%)	*S*p(*S*p*S*p/*S*p*S*p*S*p) yield (%)
ssDNA*-4	83.52 ± 2.60	88.97 ± 2.62
ssDNA*-2PS	-	51.10 ± 4.70
ssDNA*-3PS	-	39.84 ± 3.58

Numerical information is expressed as average ± stdev

All experiments were performed three times

[#]Data refer to the analysis in Fig. 4

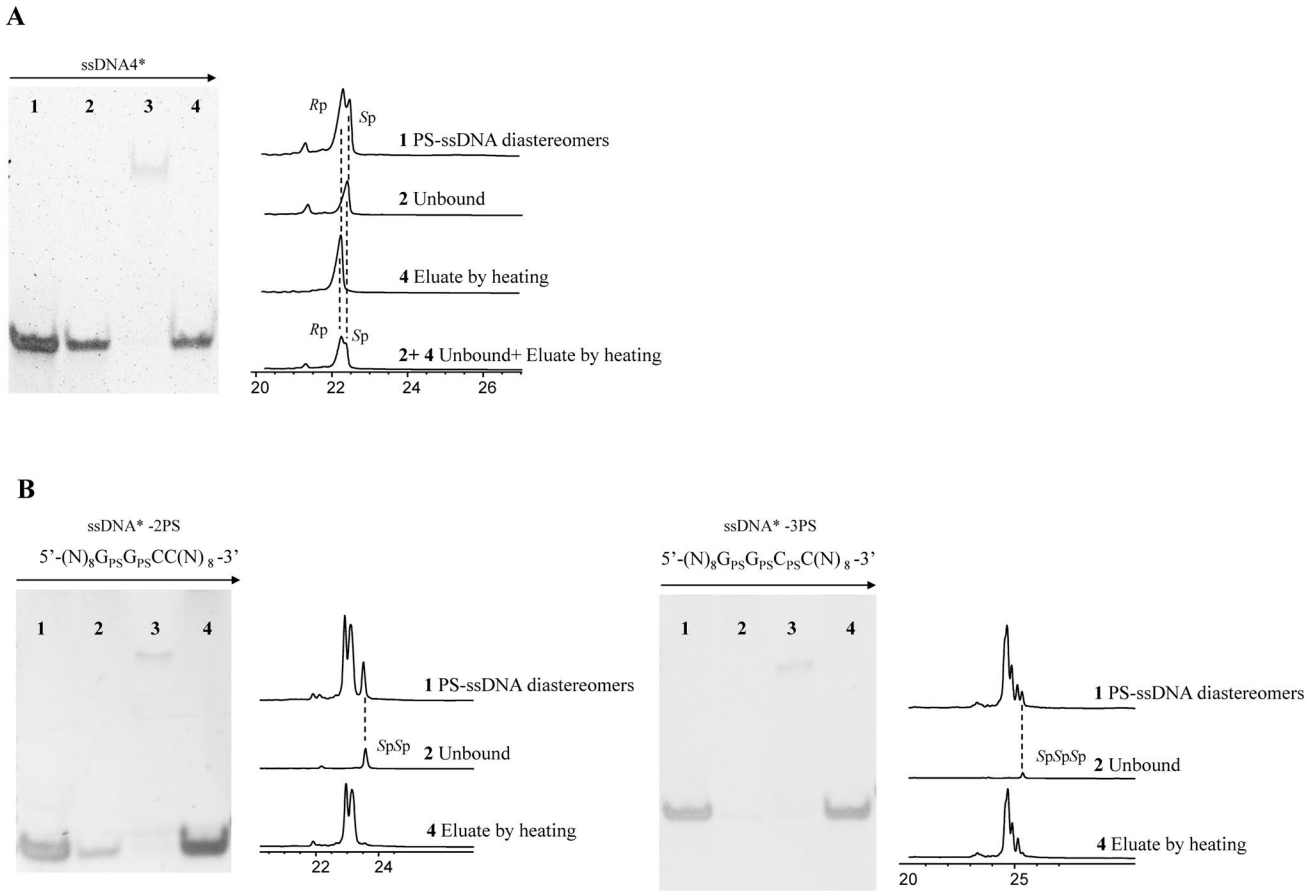

Fig. 4 **A** Effectiveness of SPOIS for separating synthetic PS-ON stereoisomers that co-elute in HPLC by anion-exchange column. Left panel shows the electrophoretic analysis of different fractions of PS-ONs purified by SPOIS. Lane 1, ssDNA PS-ON diastereomers; lane 2, unbound fraction corresponding to purified *S*p PS-ONs after SPOIS step 2a (Fig. 2A); lane 3, fraction eluted by 500 mM imidazole and corresponding to *R*p PS-ONs bound by SBD after step 3; lane 4, supernatant of fraction in lane 3 that was heated at 60 °C for 10 min, followed by centrifugation, and corresponding to purified *R*p PS-ONs. Right panel shows the HPLC profile of these fractions; 2 + 4 (lower part of panel) is a mixture of purified *S*p and *R*p used to show the closeness of the two peaks generated by the stereoisomers. **B** Effectiveness of SPOIS for purification of PS-ONs bearing two (left panel) and three (right panel) tandem PS sites. "PS" in red represents the phosphoromonothioate group. Fraction samples are the same as in panel A

1996). Nine SBDs were identified as thermolabile: #5, #20, #24, #25, #29, #32, #39, #65, and #74 (Table S3).

With EMSAs, PS-ONs with five consensus core sequences in the forms of hemi-dsDNA and ssDNA (sequences shown in Table S1) were used to measure the binding affinity of the 29 SBDs, and based on these EMSA results for the thermolabile proteins, SBDs #5 and #32 had low affinity to ssPS-ONs; #24 had low affinity to the dsPS-ON with the sequence CCA; #25 had no affinity to dsPS-ONs with sequences CCA and GATC; #29 bound the dsON with the sequence GAAC; #39 could not discern PS-ONs from ONs for all five sequences, and #74 might be incorrectly annotated as an SBD homolog as it barely bound any of the PS-ONs and ONs. Only #20 and #65 could distinguish PS-ONs from ONs with relatively high affinity and sequence flexibility. SBD #65, which also showed an obvious binding affinity for PS-RNA (Figure S11), was named SBD_{Ped} (1–170 aa, Accession No. WP_088299980.1) based on its microbial source, *Pedobacter* sp. AJM.

SBD_{Ped} was used to replace SBD_{Ana} in SPOIS, and we named the resulting new system SPOIS-II (Fig. 5A). In SPOIS-II, the magnetic bead-bound SBD_{Ped} can be directly denatured after heat treatment (step 3, Fig. 5A), leaving the denatured SBD_{Ped} still bound to the magnetic beads via His-Ni–NTA pairing (Fig. 5B). Therefore, the *R*p PS-ONs can be easily recovered just by transferring the liquid phase upon magnetic adsorption and heating (step 4, Fig. 5A). With SPOIS-II, the yield of *R*p PS-ONs was *ca.* 85% when heat treatment was performed at the optimal temperature of 85 °C (Figure S12) for 10 min, in a sharp contrast to the yield of 5% if SBD_{Ped} was replaced with SBD_{Ana} under the same conditions for SPOIS-II (Fig. 5C). In comparison, when heated without the magnetic beads, SBD_{Ped} and SBD_{Ana} were inactivated after 10 min of heat treatment at 56 °C and 60 °C,

respectively (Figure S13). The separation process for *Sp* PS-ONs remained unchanged, and the yields of *Sp* PS-ONs were *ca.* 85% in both systems. With SPOIS-II, separation of *Sp* and *Rp* PS-ONs occurred, respectively, within 5 min and 20 min, and the yield of *Rp* PS-ON using the same 20 nt synthetic PS-ON diastereomers for both SPOIS systems was *ca.* 85%.

Separation of PS substrates for DNAzyme by SPOIS-II

Phosphoromonothioate modifications are often applied to the substrate of ribozymes and DNAzymes to probe their mechanism. Upon the introduction of PS linkage at the cleavage site, the kinetics of the cleavage reactions are significantly different between *Rp* and *Sp* diastereomers (Saran et al. 2021), which is an opportunity for the application of current SPOIS system. DNAzymes are single-stranded catalytic DNA that can be screened and selected in vitro from a large pool of random DNA libraries. As an example, the Cd^{2+}-dependent RNA-cleaving DNAzyme Cd16 cleaves a modified ssDNA substrate that contains a ribonucleotide adenosine (rA) and a PS linkage immediately downstream of the rA (Fig. 6A). The *Rp* and *Sp* diastereomers of this PS substrate exhibit opposite cleavage results, necessitating isomer separation. Previously developed strategies for preparation of this *Rp* PS substrate involve the following: (i) separation of a left-side *Rp* PS isomer, followed by ligation to a right-side ON; or (ii) removal of one full-length PS-ON diastereomer substrate by *Rp*- or *Sp*-specific DNAzyme

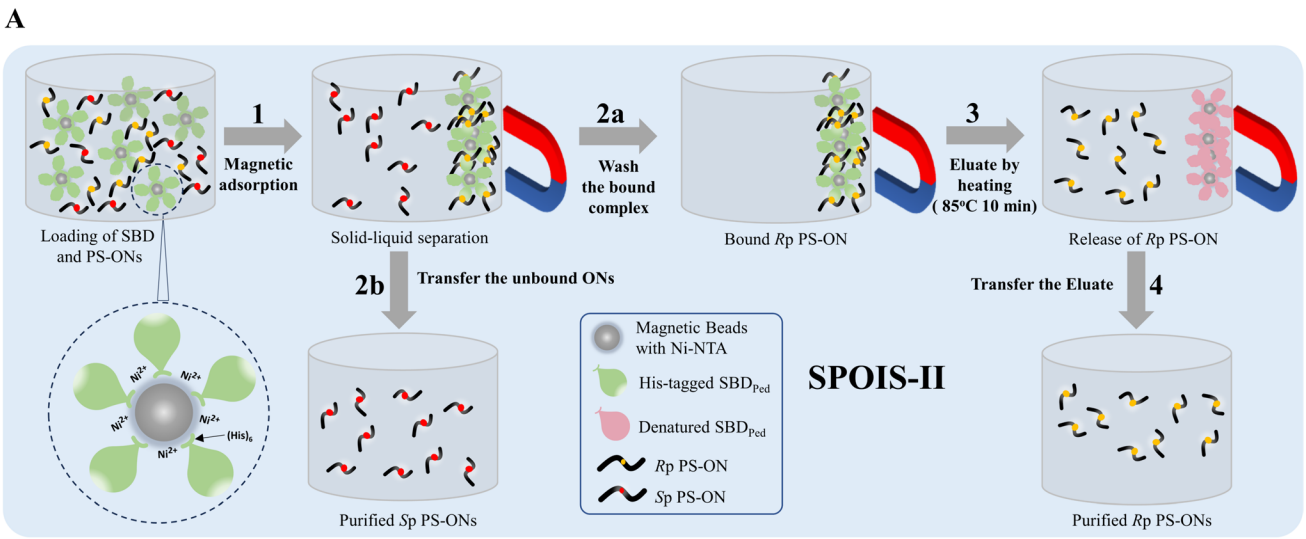

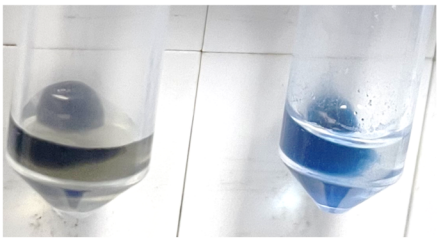

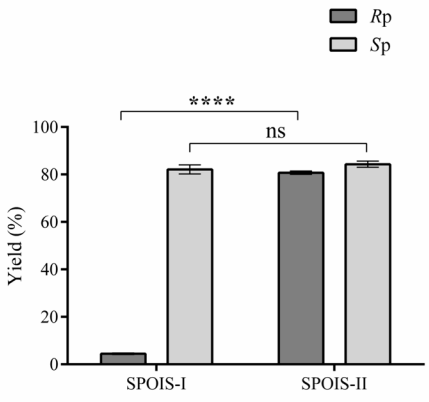

Fig. 5 Establishment of SOPIS-II based on the thermo-labile SBD_{Ped}. **A** Flowchart of the SBD_{Ped}-based SPOIS-II separation process for *Rp* and *Sp* PS-ON stereoisomers. **B** Color reaction of the magnetic beads/SBD_{Ped} (right tube) remaining after step 4 of panel A with 400 µL CBB Staining Solution (Tiangen) added. The blue color indicates the presence of protein. The left tube contains the Ni–NTA magnetic bead control without SBD_{Ped} loaded. **C** Comparison of the yields of *Rp* and *Sp* PS-ONs with SBD_{Ana} and SBD_{Ped} after heating in step 3 (panel A). The *Rp* PS-ONs bound by SBD_{Ana} or SBD_{Ped} were heated and released at 85 °C for 15 min, and the yields were compared based on HPLC analysis. Error bars represent the standard deviations of yields performed in triplicate. A t-test was applied for comparison: ns, no significance; ****$p < 0.0001$

digestion (Huang and Liu 2015). For SPOIS-II, 1 nmol of a 24 nt PS substrate for the Cd16 DNAzyme (Huang and Liu 2015) was synthesized and separated. Within 20 min, 0.41 nmol *S*p isomers and 0.52 nmol *R*p isomers were obtained (Fig. 6A, right panel). As shown in Fig. 6B, about 80% of the purified *R*p isomers were cleaved by Cd16, as compared to 25% for the *S*p substrates (Fig. 6B), which is consistent with the cleavage efficiency of the diastereomers purified by multiple separations of HPLC or *R*p/*S*p-specific DNAzyme digestion but the purification of SPOIS is with lower labor and less time costs. The above results fully confirm the high utility and value of the SOPIS system for diastereomer separation of varied PS-ONs, especially the PS substrate of DNAzymes and ribozymes.

Discussion

SBD_{Ana} and SBD_{Ped} displayed a higher affinity for ssPS-ONs when compared to SBD_{Hga} and SBD_{Spr} (Fig. 1, Figure S1B); however, the consensus sequence bearing the PS linkage can impact binding affinity as some SBDs displayed strong sequence specificity for binding PS dsDNA. Given that we only tested five natural core consensus sequences when evaluating the sequence specificity of SBD_{Ana} and SBD_{Ped}

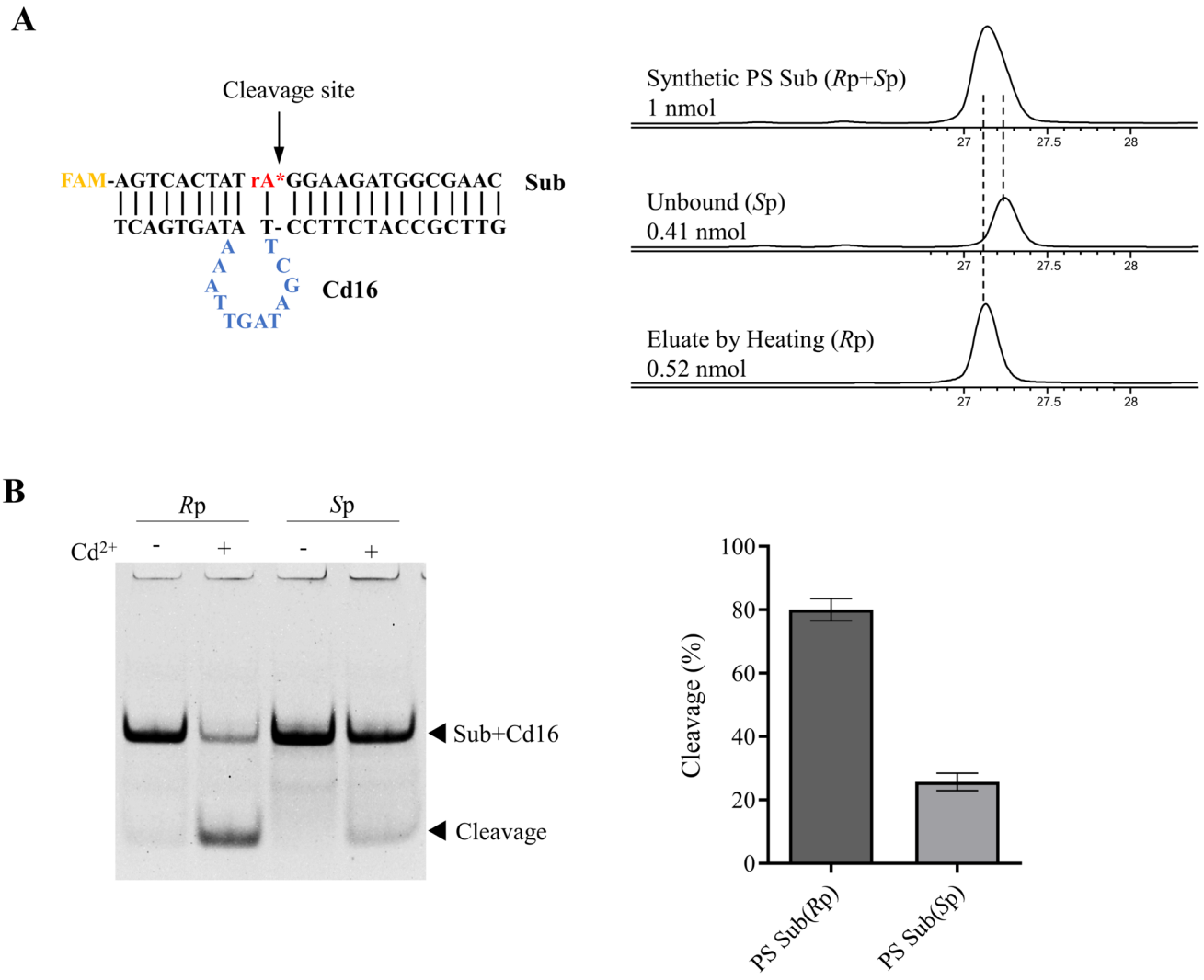

Fig. 6 Rapid separation of the PS-ON stereoisomer substrate of DNAzyme Cd16 by SPOIS-II. **A** Cd16 target sequence and HPLC analysis of synthetic PS-ONs and *R*p and *S*p isomers purified by SPOIS-II. Left panel: rA in red, ribonucleotidyl adenosine; FAM, carboxyfluorescein; "*", phosphoromonothioate group; Cd16, the DNAzyme. Right panel: synthetic PS-ON diastereomers co-elute as a single peak; unbound and eluate by heating correspond to *S*p and *R*p PS-ONs, respectively. **B** Electrophoretic analysis of the cleavage products of the PS-ON stereoisomer by Cd16. The cleavage percentage of two PS-ONs is shown on the right. Error bars represent the standard deviations of yields performed in triplicate

(Table S3), we cannot exclude the possibility that both SBDs have some sequence specificity in PS-DNA binding. In order to achieve high yields of stereo-pure isomers using SPOIS, the binding affinity of SBD_{Ana} or SBD_{Ped} toward a particular PS-ON can first be evaluated simply by EMSA.

Elution of *R*p isomers from SBD_{Ana} was a substantial challenge in SPOIS. Although heat treatment at 60 °C for 10 min could inactivate the PS-binding activity of SBD_{Ana} (Figure S5), heat treatment of the magnetic beads/SBD_{Ana}/*R*p PS-ON complex at 95 °C for 30 min still only recovered less than 10% of *R*p PS-ONs as compared to 85% by the method using imidazole elution (Figure S4). We deduce that immobilization of His-tagged SBD_{Ana} on the magnetic beads stabilizes the activity of SBD_{Ana} and that heat treatment at 95 °C may detach the *R*p PS-ONs from the SBD_{Ana}. However, following heat treatment, a short centrifugation and magnetic adsorption were performed at room temperature, which might have resulted in a sharp decrease in the temperature of the SPOIS system, allowing for re-association of the PS-ONs and SBD_{Ana}. Therefore, the immobilization of SBD_{Ana} may significantly improve its thermostability. Although immobilization of SBD_{Ped} onto beads enhanced the thermostability of SBD_{Ped}, a result supported by the lower denaturation temperature in the absence of beads (Figure S13), heat treatment of the magnetic beads/SBD_{Ped} /*R*p PS-ON complex at 85 °C for 10 min efficiently released the *R*p PS-ONs (Fig. 5C); notably, SBD_{Ped} was not detached from the beads after this treatment (Fig. 5B), implying that SBD_{Ped} is denatured but the attached His-tag remains firmly bound to the Ni–NTA. Since two steps in SPOIS-I (imidazole-heat elution and desalting) are not necessary for SPOIS-II, thus SPOIS-II saves time and materials.

All reported SBDs recognize PS in an *R*p-specific way, and the mechanisms underlying stereospecificity have been explained based on the complex structure of SBDs with their respective PS-ONs (Liu et al. 2018). In addition to interactions with the sulfur atom in PS-ONs, SBDs bond with the phosphodiester backbone and bases adjacent to the PS linkage (Figure S1C, Figure S8). These interactions may also be necessary for firm binding of PS-ONs by SBD_{Ana}, as SBD_{Ana} could not capture the short PS-ONs with a length below 4 nt from the liquid phase (Figure S7). Moreover, some approved siRNAs such as givosiran, lumasiran, inclisiran, and vuttrisiran each carry two PS sites at the 3′ and 5′ ends. Thus, half of these siRNA diastereomers can be separated by SPOIS relying on SBD binding to the inner PS linkage but with the last PS linkage in mixed stereoisomers. This purification alters the isomeric composition of the siRNA, affecting its pharmacological properties to some extent(Jahns et al. 2022). The SBD_{Ana} could bind PS-ONs longer than 70 nt (Figure S10) in EMSA but the immobilized SBD_{Ana} could not separate them from the liquid phase to the solid phase magnetic bead complex in SPOIS-I. A possibility is that the bound longer ONs might introduce space hindrance against the access to adjacent SBD for other ON molecules, leading to a decreased yield of *R*p isomers of the longer PS-ONs.

Based on the specific recognition and binding of SBD_{Ana}/SBD_{Ped} to PS-DNA and PS-RNA in the *R*p configuration, the SPOIS system can be used to separate PS-DNA and PS-RNA diastereomers of 4 nt to 50 nt in length with yields of 60–90%. The current SPOIS system is more suitable for diastereomer separation of phosphoromonothioate ONs, such as substrates for DNAzyme and ribozymes. For ONs with multiple PS sites, due to the nature of SBD as each well-located *R*p PS linkage can be bound by SBD, the current SPOIS cannot achieve the complete diastereomer separation of ONs with multiple PS sites. Nevertheless, for ONs with PS modifications at each linkage, purification of SPOIS can help to remove the uniform *S*p configuration from their fractions, which may influence their pharmacological properties. Moreover, rational design and adaptation of SBDs, e.g., tandem SBDs, may be a potential bioenzymatic way to separate diastereomers of ONs with more PS sites.

The diastereomer separation based on chromatography mainly relies on the polarity difference of diastereomers (Frederiksen and Piccirilli 2009), which imposes additional limitations on oligonucleotide length and sequence, phosphorothioate position, column type, buffer composition, and other parameters. In comparison, SPOIS is a more universal way without individually customized separation procedure for a given PS-ON. What is more, the lower costs of labor and time and the no need for bulky instrumentation make it an easy and fast bioenzymatic method for diastereomer separation of PS-ONs.

Supplementary Information The online version contains supplementary material available at https://doi.org/10.1007/s00253-024-13283-3.

Acknowledgements The funders had no role in study design, data collection and interpretation, or the decision to submit the work for publication.

Author contribution FG: experiment design; investigation (lead); writing—original draft. YW: investigation (supporting). JL: investigation (supporting). HY: investigation (supporting). GL: resources (supporting). ZD: funding acquisition (supporting). XH: funding acquisition (lead); supervision (lead); writing—review and editing.

Funding This work was supported by grants from the National Key Research and Development Program of China (2020YFA0907200); the National Natural Science Foundation of China (32170047, 31871250, 31670034); the Shanghai Pilot Program for Basic Research—Shanghai Jiao Tong University (21TQ1400204); and the Natural Science Foundation of Shanghai (22ZR1430100).

Data availability The data underlying this article are available in the article and in its online supplementary data.

Declarations

Ethics approval No human or animal subjects were used in this study.

Conflict of interest The authors declare no competing interests.

References

Brautigam CA, Steitz TA (1998) Structural principles for the inhibition of the 3'-5' exonuclease activity of *Escherichia coli* DNA polymerase I by phosphorothioates. J Mol Biol 277(2):363–377. https://doi.org/10.1006/jmbi.1997.1586

Bryant FR, Benkovic SJ (1979) Stereochemical course of the reaction catalyzed by 5'-nucleotide phosphodiesterase from snake venom. Biochemistry 18(13):2825–2828. https://doi.org/10.1021/bi00580a022

Cancado ELR, VilasBoas LS, AbrantesLemos CP, Novo NF, Porta G, DaSilva LC, Laudanna AA (1996) Heat serum inactivation as a mandatory procedure for antiactin antibody detection in cell culture. Hepatology 23(5):1098–1104. https://doi.org/10.1002/hep.510230525

Eckstein F (1985) Nucleoside phosphorothioates. Annu Rev Biochem 54:367–402. https://doi.org/10.1146/annurev.bi.54.070185.002055

Eckstein F (2014) Phosphorothioates, essential components of therapeutic oligonucleotides. Nucleic Acid Ther 24(6):374–387. https://doi.org/10.1089/nat.2014.0506

Egli M, Manoharan M (2023) Chemistry, structure and function of approved oligonucleotide therapeutics. Nucleic Acids Res 51(6):2529–2573. https://doi.org/10.1093/nar/gkad067

Enmark M, Bagge J, Samuelsson J, Thunberg L, Ornskov E, Leek H, Lime F, Fornstedt T (2020) Analytical and preparative separation of phosphorothioated oligonucleotides: columns and ion-pair reagents. Anal Bioanal Chem 412(2):299–309. https://doi.org/10.1007/s00216-019-02236-9

Enmark M, Harun S, Samuelsson J, Ornskov E, Thunberg L, Dahlen A, Fornstedt T (2021) Selectivity limits of and opportunities for ion pair chromatographic separation of oligonucleotides. J Chromatogr A 1651:462269. https://doi.org/10.1016/j.chroma.2021.462269

Frederiksen JK, Piccirilli JA (2009) Separation of RNA phosphorothioate oligonucleotides by HPLC. Methods Enzymol 468:289–309. https://doi.org/10.1016/S0076-6879(09)68014-9

Guo M, Yu D, Iyer RP, Agrawal S (1998) Solid-phase stereoselective synthesis of 2'-O-methyl-oligoribonucleoside phosphorothioates using nucleoside bicyclic oxazaphospholidines. Bioorg Med Chem Lett 8(18):2539–2544. https://doi.org/10.1016/s0960-894x(98)00450-8

Hu W, Yang B, Xiao Q, Wang Y, Shuai Y, Zhao G, Zhang L, Deng Z, He X, Liu G (2023) Characterization of a promiscuous DNA sulfur binding domain and application in site-directed RNA base editing. Nucleic Acids Res 51(19):10782–10794. https://doi.org/10.1093/nar/gkad743

Huang PJ, Liu J (2015) Rational evolution of Cd^{2+}-specific DNAzymes with phosphorothioate modified cleavage junction and Cd^{2+} sensing. Nucleic Acids Res 43(12):6125–6133. https://doi.org/10.1093/nar/gkv519

Iwamoto N, Butler DCD, Svrzikapa N, Mohapatra S, Zlatev I, Sah DWY, Meena SSM, Lu G, Apponi LH, Frank-Kamenetsky M, Zhang JJ, Vargeese C, Verdine GL (2017) Control of phosphorothioate stereochemistry substantially increases the efficacy of antisense oligonucleotides. Nat Biotechnol 35(9):845–851. https://doi.org/10.1038/nbt.3948

Jahns H, Taneja N, Willoughby JLS, Akabane-Nakata M, Brown CR, Nguyen T, Bisbe A, Matsuda S, Hettinger M, Manoharan RM, Rajeev KG, Maier MA, Zlatev I, Charisse K, Egli M, Manoharan M (2022) Chirality matters: stereo-defined phosphorothioate linkages at the termini of small interfering RNAs improve pharmacology in vivo. Nucleic Acids Res 50(3):1221–1240. https://doi.org/10.1093/nar/gkab544

Koziolkiewicz M, Krakowiak A, Kwinkowski M, Boczkowska M, Stec WJ (1995) Stereodifferentiation–the effect of P chirality of oligo(nucleoside phosphorothioates) on the activity of bacterial RNase H. Nucleic Acids Res 23(24):5000–5005. https://doi.org/10.1093/nar/23.24.5000

Liu G, Fu W, Zhang Z, He Y, Yu H, Wang Y, Wang X, Zhao YL, Deng Z, Wu G, He X (2018) Structural basis for the recognition of sulfur in phosphorothioated DNA. Nat Commun 9(1):4689. https://doi.org/10.1038/s41467-018-07093-1

Murakami A, Tamura Y, Wada H, Makino K (1994) Separation and characterization of diastereoisomers of antisense oligodeoxyribonucleoside phosphorothioates. Anal Biochem 223(2):285–290. https://doi.org/10.1006/abio.1994.1586

Oka N, Yamamoto M, Sato T, Wada T (2008) Solid-phase synthesis of stereoregular oligodeoxyribonucleoside phosphorothioates using bicyclic oxazaphospholidine derivatives as monomer units. J Am Chem Soc 130(47):16031–16037. https://doi.org/10.1021/ja805780u

Potter BV, Eckstein F (1984) Cleavage of phosphorothioate-substituted DNA by restriction endonucleases. J Biol Chem 259(22):14243–14248. https://doi.org/10.1016/s0021-9258(18)89884-2

Potter BVL, Connolly BA, Eckstein F (1983) Synthesis and configurational analysis of a dinucleoside phosphate isotopically chiral at phosphorus - stereochemical course of *Penicillium-Citrum* nuclease P1 reaction. Biochemistry 22(6):1369–1377. https://doi.org/10.1021/bi00275a008

Putney SD, Benkovic SJ, Schimmel PR (1981) A DNA fragment with an alpha-phosphorothioate nucleotide at one end is asymmetrically blocked from digestion by exonuclease III and can be replicated in vivo. Proc Natl Acad Sci U S A 78(12):7350–7354. https://doi.org/10.1073/pnas.78.12.7350

Roberts TC, Langer R, Wood MJA (2020) Advances in oligonucleotide drug delivery. Nat Rev Drug Discov 19(10):673–694. https://doi.org/10.1038/s41573-020-0075-7

Saran R, Huang ZC, Liu JW (2021) Phosphorothioate nucleic acids for probing metal binding, biosensing and nanotechnology. Coordin Chem Rev 428:213624. https://doi.org/10.1016/j.ccr.2020.213624

Stec WJ, Karwowski B, Boczkowska M, Guga P, Koziolkiewicz M, Sochacki M, Wieczorek MW, Blaszczyk J (1998) Deoxyribonucleoside 3′-*O*-(2-thio- and 2-oxo-"spiro"-4,4-pentamethylene-1,3,2-oxathiaphospholane)s: monomers for stereocontrolled synthesis of oligo(deoxyribonucleoside phosphorothioate)s and chimeric PS/PO oligonucleotides. J Am Chem Soc 120(29):7156–7167. https://doi.org/10.1021/ja973801j

Wilk A, Grajkowski A, Phillips LR, Beaucage SL (2000) Deoxyribonucleoside cyclic *N*-acylphosphoramidites as a new class of monomers for the stereocontrolled synthesis of

oligothymidylyl- and oligodeoxycytidylyl-phosphorothioates. J Am Chem Soc 122(10):2149–2156. https://doi.org/10.1021/ja991773u

Yu D, Kandimalla ER, Roskey A, Zhao Q, Chen L, Chen J, Agrawal S (2000) Stereo-enriched phosphorothioate oligodeoxynucleotides: synthesis, biophysical and biological properties. Bioorg Med Chem 8(1):275–284. https://doi.org/10.1016/s0968-0896(99)00275-8

Yu H, Liu G, Zhao G, Hu W, Wu G, Deng Z, He X (2018) Identification of a conserved DNA sulfur recognition domain by characterizing the phosphorothioate-specific endonuclease SprMcrA from *Streptomyces pristinaespiralis*. Mol Microbiol 110(3):484–497. https://doi.org/10.1111/mmi.14118

Yu H, Li J, Liu G, Zhao G, Wang Y, Hu W, Deng Z, Wu G, Gan J, Zhao YL, He X (2020) DNA backbone interactions impact the sequence specificity of DNA sulfur-binding domains: revelations from structural analyses. Nucleic Acids Res 48(15):8755–8766. https://doi.org/10.1093/nar/gkaa574

Zhou X, He X, Liang J, Li A, Xu T, Kieser T, Helmann JD, Deng Z (2005) A novel DNA modification by sulphur. Mol Microbiol 57(5):1428–1438. https://doi.org/10.1111/j.1365-2958.2005.04764.x